Fottea, Olomouc, 25(1): 68–80, 2025
DOI: 10.5507/fot.2024.010

Trebouxia barrenoae sp. nov. (*Trebouxiophyceae*, *Chlorophyta*), a new lichenized microalga widespread in temperate ecosystems

Tamara Pazos[1*], Patricia Moya[1], Isaac Garrido–Benavent[2], César D. Bordenave[1], Ayelén Gazquez[3] & Salvador Chiva[1]

[1]*Instituto Cavanilles de Biodiversidad y Biología Evolutiva (ICBiBE)– Botànica, Universitat de València, C/ Dr. Moliner, 50, E–46100 Burjassot, València, Spain; *Corresponding author e–mail: tamara.pazos@uv.es*
[2]*Departament de Botànica i Geologia, Universitat de València, C/ Dr. Moliner, 50, E–46100 Burjassot, València, Spain*
[3]*Instituto de Biotecnología y Biomedicina (BIOTECMED), Universitat de València, E–46100 Burjassot, València, Spain*

Abstract: The genus *Trebouxia* includes the most widespread green microalgae inhabiting lichen thalli worldwide. Nonetheless, the vast majority of species–level phylogenetic lineages within this genus lack a formal taxonomic description and, to date, only 31 species have been accepted. In this study, we utilized an integrative taxonomic approach to describe the new species *Trebouxia barrenoae* Pazos, Chiva, Garrido–Benavent et Moya, a frequent symbiont in different lichens which is phylogenetically circumscribed to *Trebouxia* clade S. The ultrastructural features of the new microalga were studied through light, confocal, and electron microscopies; phylogenetic, physiological, and ecological niche analyses were carried out to characterize this new taxon as well. Our findings revealed a more frequent association of *T. barrenoae* sp. nov. with vegetatively reproducing lichens that thrive in temperate forest habitats and showed a preference for those growing on acidic substrates. The description of this species fosters progress in the systematics and taxonomy of the genus *Trebouxia* and enhances precise characterization of lichen phycobionts.

Key words: chlorophyll fluorescence, epiphytic lichen, niche hypervolume, photobiont, symbiosis, taxonomic integrative approach, transmission electron microscopy (TEM)

Introduction

Trebouxia Puymaly (*Trebouxiaceae* Friedl) is a globally distributed green microalgal genus that encompasses terrestrial species, which frequently take part in mutualistic symbioses involving a wide range of lichen–forming fungi across diverse ecosystems (e.g., Miadlikowska et al. 2014; Muggia et al. 2018; de Carolis et al. 2022; Veselá et al. 2024; Grube 2024). Despite partnering with ca. 20% of all known species of lichenized fungi (Rambold et al. 1998; Muggia et al. 2020; Nelsen et al. 2021; Kosecka et al. 2022), only 31 *Trebouxia* species have a formal taxonomic description so far, and, frequently, new lichenized lineages are reported (e.g., Friedl 1989; Leavitt et al. 2015; Muggia et al. 2020; Barreno et al. 2022; Garrido–Benavent et al. 2022; Kosecka et al. 2022; Guiry & Guiry 2024). Recently, Muggia et al. (2020) reappraised species diversity and evolutionary relationships and generated a multi–locus phylogenetic reference framework in which to base future research in *Trebouxia* systematics and taxonomy. Furthermore, their study revealed the division into four main *Trebouxia* clades previously reported by Helms et al. (2001): clade A (named after *T. arboricola*,), clade C (after *T. corticola*), clade I (after *T. impressa*) and clade S (after *T. simplex*). Shortly after, Xu et al. (2020) segregated some *Trebouxia* lineages from clade S, specifically those associating with the lichen–forming fungus *Cetrariella delisei* (Bory ex Schaer.) Kärnefelt et A. Thell, to a fifth, well–supported clade, named as *Trebouxia* clade 'D' after the lichenized fungal specific epithet "*delisei*". Unfortunately, most putative species–level lineages within those clades lack a taxonomical description, which constitutes an impediment when communicating results of biodiversity and ecological interactions in lichens.

A recent study by Pazos et al. (2024, submitted) addressing the genetic diversity of the myco– and phycobionts and their interactions in an epiphytic lichen community from forest ecosystems in the eastern Iberian Peninsula reported a further undescribed taxon included in the genus *Trebouxia*. This microalga, which belonged

to the *Trebouxia* clade S and therefore was provisionally named as *Trebouxia* sp. S28, was the most frequent photosynthetic partner in the analyzed community. In the present study we formally describe this new lichenized *Trebouxia* following an integrative taxonomic approach that combines traditional morphological descriptions (Archibald 1975; Friedl 1989; Ettl & Gärtner 2014) together with molecular phylogenetics, ultrastructural, physiological and ecological data (e.g., Rivas–Martínez et al. 2017; Molins et al. 2018; Muggia et al. 2018; Škaloud et al. 2018; Barreno et al. 2022; Garrido–Benavent et al. 2022).

Material and methods

Taxon sampling. The list of studied lichen specimens that were collected during 2022 in five localities across forest ecosystems located in the eastern Iberian Peninsula was reported in Moya et al. (2023) and Pazos et al. (2024, submitted). The number of lichen thalli that hosted the new microalga species (i.e., *Trebouxia* sp. S28) was 61, of which 39 corresponded with *Pseudevernia furfuracea* (L.) Zopf, 19 with *Parmelia serrana* A. Crespo, M.C. Molina et D. Hawksw., two with *Xanthoria parietina* (L.) Th. Fr. and one with *Anaptychia ciliaris* (L.) A. Massal.

Microalgae isolation and culturing. One specimen of *P. furfuracea* collected in El Toro (Castelló, Spain) was selected for algal isolation following the method described in Chiva et al. (2021). Grown unialgal colonies were subcultivated on liquid Bold's Basal Media Petri dishes (BBM, Bold 1949; Bischoff & Bold 1963), and a volume of 50 µl was plated onto solid BBM for 21 days. After this period, a single grown colony was retrieved to be (1) used for morphological and physiological analyses, and (2) stored as living strain at the Symbiotic Algal Collection of the Universitat de València (strain code ASUV143) and at the Spanish Algae Bank ("Banco Español de Algas", strain code BEA2100B). Light/darkness time cycles and light intensity in the growth chambers for the viable cultures also followed Chiva et al. (2021).

DNA extraction, PCR amplification, purification, and sequencing. Total genomic DNA of the unialgal culture was isolated using the DNeasy Plant Mini Kit (Qiagen, Hilden, Germany) following the manufacturer's instructions. Four algal loci were then amplified: the green microalgal barcode nuclear ribosomal Internal Transcribed Spacer (nrITS), with the primer pair nr–SSU–1780 (Piercey–Normore & DePriest 2001) and ITS4T (Kroken & Taylor 2000); the chloroplast, protein–coding ribulose–1,5–bisphosphate carboxylase/oxygenase large subunit (rbcL), with the primer pair rbcL151f/rbcL986R (Nelsen et al. 2011); the mitochondrial, protein–coding cytochrome c oxidase (cox2), with the primer pair COXIIf2/COXIIr (Lindgren et al. 2014); and a region of the chloroplast LSU rDNA gene (primer pair 23SU1/23SU2, del Campo et al. 2010). PCR reactions for nrITS, cox2 and LSU rDNA started with a denaturalization step of two min at 94 °C, followed by 30 cycles of 30 s at 94 °C, 45 s at 56 °C and one min at 72 °C, and they ended with a final elongation step at 72 °C for five min. For the rbcL, we followed Nelsen et al. (2011). PCR products were then visualized on 1% agarose gels and purified using the NZYGelpure kit (NZYTECH). Sanger sequencing of purified PCR products was performed with an ABI 3100 Genetic analyzer using the ABI BigDye TM Terminator Cycle Sequencing Ready Reaction Kit (Applied Biosystems, Foster City, California, USA) at StabVida (Portugal). Sequence edition and consensus assembly of forward and reverse reads were performed using SnapGene Viewer 7.0.2 (GSL Biotech. 2023).

Assembly of sequence datasets, alignments, and phylogenetic analyses. Sequence data from the nrITS, cox2 and rbcL markers were employed for inferring three different single–locus phylogenetic trees. Species and specimen selection for assembling sequence datasets was based on Muggia et al. (2020). For phylogenetic tree comparison, only specimens with all three markers (nrITS, cox2 and rbcL) were included in the analyses. An LSU sequence dataset was not compiled due to the lack of sequence data for most lineages within *Trebouxia* clade S. The ingroup consisted of samples of the new *Trebouxia* sp. S28, as well as *T. angustilobata*, *T. simplex* and *T. suecica* and sequences obtained from still undescribed species–level lineages, which are generally named as *Trebouxia* sp. followed by S and a two–digit numeral (Leavitt et al. 2015; Muggia et al. 2020). The outgroup (used to root the phylogenetic tree) consisted of a few specimens representing undescribed species belonging to *Trebouxia* clade A (see Supplementary Table S1).

Alignments for the three markers were built separately using MAFFT v. 7.505 (Katoh et al. 2002; Katoh & Standley 2013), with the FFT–NS–I x1000 algorithm, the 200PAM / k = 2 scoring matrix, a gap open penalty of 1.5 and an offset value of 0.123. Resulting alignments were manually edited to trim ends of longer sequences and to annotate (1) partitions within the whole nrITS region and (2) codon positions in the protein–coding cox2 and rbcL. Phylogenetic inferences were then made following two approaches: Maximum Likelihood (ML) and Bayesian Inference (BI). ML tree estimations were carried out with RAxML (Stamatakis 2006; Stamatakis et al. 2008) as implemented in the CIPRES Science Gateway (Miller et al. 2010), using the GTRGAMMA as the nucleotide substitution model for the defined sequence data partitions. One thousand rapid bootstrap pseudoreplicates were conducted to evaluate nodal support. We first generated single–locus trees to test for topological incongruence among them, assuming bootstrap values ≥70 % as significant for conflicting relationships among the same set of taxa (Mason–Gamer & Kellogg 1996). Then, and because no conflicts were found, a multi–locus RAxML tree was constructed. Before constructing a multi–locus Bayesian tree, PartitionFinder v. 1.1.1 (Lanfear et al. 2012) was used to find the optimal evolutionary nucleotide substitution and partition schemes (Supplementary Table S2). The BI phylogenetic reconstruction was conducted with the program MrBayes v. 3.2.7 (Ronquist et al. 2012), with two parallel, simultaneous four–chain runs executed over 5×10^7 generations starting with a random tree, and sampling after every 500th step. The first 25% of data was discarded as burn–in, and the 50% majority–rule consensus tree and corresponding posterior probabilities (PP) were calculated from the remaining trees. Chain convergence was assessed ensuring that the potential scale reduction factor (PSRF) approached 1.00 and that the average standard deviation of split frequencies (ASDSF) values fell below 0.005. Tree nodes with bootstrap support (BS) values higher than 70% and PP equal or higher than 0.95 were regarded as significantly supported. Trees were drawn with FigTree (http://tree.bio.ed.ac.uk/software/figtree/) and InkScape (https://inkscape.org) was used for artwork.

Multi–microscopic approach to characterize the new *Trebouxia*. Light microscopy (LM), confocal laser scanning microscopy (CLSM) and transmission electron microscopy (TEM) were performed to conduct a comprehensive morphological analysis of the new *Trebouxia* species based on unialgal isolation cultures (ASUV143) on their 21st day of cultivation at 20° C. LM observations were done using a Nikon Eclipse E–800 microscope, whereas photographs were taken with a Nikon DS–Ri1 camera (ICBIBE Microscopy Service). For CLSM, the strain was processed as described in Bordenave et al. (2022). TEM was employed to investigate the ultrastructural

Fottea, Olomouc, 25(1): 68–80, 2025
DOI: 10.5507/fot.2024.010

characteristics of the new *Trebouxia* both in culture and symbiotic state. Cells were fixed and dehydrated as described in Molins et al. (2018). Samples were subsequently embedded in Spurr's resin according to the manufacturer's instructions. After embedding, ultra–thin sections measuring 80 nm in thickness were cut using a diamond knife (DIATOME ultra 45°) and mounted on 100 mesh copper grids, as described in Bordenave et al. (2022). These sections were then stained with a solution of 10% uranyl acetate and 0.1% lead citrate utilizing the "Synaptek Grid–Stick Kit". Finally, sections were examined at 80 kV using a JEOL JEM–1010 microscope (Jeol, Peabody, MA, USA), and images were captured employing an Olympus MegaView III camera and subsequently processed using the Fiji distribution of ImageJ (Schindelin et al. 2012). Representative images of the new isolated microalga were acquired at the SCSIE (Universitat de València).

Growth conditions for physiological analyses. Prior to treatments, and to know the cell concentration of the isolated microalgal strain, one culture was filtered through a 50 µm pore filter (Partec, Celltrics) and counted in the Neubauer chamber. Subsequently, the cell concentration was readjusted to 5.0×10^7 cells.µl^{-1}. 50 µl of filtered cell suspension were applied directly over solid 3N–BBM (Gasulla *et al.* 2010). Supplemented with glucose 20 gl^{-1} and casein hydrolysate 10 gl^{-1}. For treatments, six sets of twelve colony replicates each were prepared: 32 photosynthetically active radiation (PAR) and 15 ºC, 32 PAR and 20 ºC, 50 PAR and 15 ºC, 50 PAR and 20 ºC, 90 PAR and 15 ºC, and 90 PAR and 20 ºC. All treatments lasted 21 days and a 12 h photoperiod with upper light was applied. Colony growth and chlorophyll fluorescence measurements were done, for consistency, between 2–4 hours after the light period started.

Colony growth measurements. During the treatment days, colony growth was measured every day using a photographic, non–destructive method that allowed us to follow each individual colony over time. Images were taken at fixed distance with a Canon EOS 2000D digital camera (Canon, Ōta City, Tokyo, Japan), analyzed with Fiji distribution of ImageJ (Schindelin et al. 2012) and integrated densities (IntDen) were acquired for each image of each colony. For each measurement of IntDen the corresponding background value was subtracted from the colony value. IntDen values were then used for fitting three parameter logistic least square growth curve models using R–Studio v. 2022.02.0 (R studio Team 2021) and R v. 4.1.2 statistical software packages (R Core Team 2021). The model is given by the following equation:

$$y = \kappa / (1 + \exp(-r * (t - t_{mid})),$$

where y is area or integrated density at time t; κ is the carrying capacity of the population, the maximum colony size; t_{mid} is the time at which the colony reaches half of its maximum size; and r is the intrinsic growth rate. After curve fitting was performed, maximum growth rate (μ_m) was calculated as the slope at the midpoint as r*κ/4, the duration of the lag phase (t_{lag}) was estimated as the time at which the line passing through (t_{mid}, κ/2) with slope μ_m equals the initial inoculum $y = n_0$, and the time at which κ was reached and the stationary phase initiates (t_{stat}) was determined as the line passing through (t_{mid}, κ/2) with slope μ_m equals y = κ.

The data of growth parameters κ, r, t_{mid}, μ_m, t_{stat} and t_{lag} and chlorophyll–fluorescence parameter F_v/F_m were analyzed with two–way analysis of variance (ANOVA) using light radiation (PAR) and temperature as factors, followed by post hoc comparisons using Tukey's HSD test. The value 0.05 was considered the significance level. Calculations were performed using R v. 4.1.2 (R Core Team 2021).

Chlorophyll fluorescence fast–transient test. After 21 days of algal colony growth, transient fluorescence of PSII (Photosystem II) chlorophyll measurements were made with a fluorometer (HandyPEA, Hansatech Instruments®) according to Rachoski et al. (2015). Briefly, colonies were dark–adapted for 5 min with leaf clips. Then, leaf clips were opened, and samples were exposed during 3 s to 3500 µmol photons.m^{-2}.s^{-1} (637 nm peak wavelength). Data were analyzed by the PEA Plus software (Hansatech Instruments®) and OJIP analysis was performed (Stirbet & Govindjee 2011). F_v/F_m or maximum quantum yield of primary PSII photochemistry was used for comparison of treatments.

Microalga ecological characterization. Ecological preferences and geographic distribution of the new microalga were assessed based on our own records and metadata of sequences deposited in GenBank that could be attributed to the new *Trebouxia*. Such attribution was corroborated phylogenetically building a single–locus nrITS phylogenetic tree with RAxML that included (1) the nrITS sequence of collection ASUV143 (OK577856) which represents the new species' type (see Results section below), and (2) the first 1000 sequences obtained after conducting a BLAST search against the GenBank database and considering all hits showing a 95% or more identity match (data not shown). Based on clade placement and bootstrap support values (BP ≥ 70%), the number of sequences that could be attributed to the new *Trebouxia* was 120 (Supplementary Table S3). A map showing the geographical distribution of the new species was designed using the function map_data in R package ggplot2 (Wickham 2016).

Additionally, using all *Trebouxia* clade S sequences available in GenBank, and relying on the phylogeny inferred by Kosecka et al. (2022), we conducted a climatic niche analysis of the new *Trebouxia* species and other formally described species within *Trebouxia* clade S following Vančurová et al. (2018, 2021). For data obtained from GenBank, only entries with accurate geospatial coordinates and species affiliation were used. Climatic niche hypervolumes were therefore represented for the new *Trebouxia* (n = 94), *T. angustilobata* (n = 45), *T. simplex* (n = 63) and *T. suecica* (n = 55) (Supplementary table S4), using the Hutchinsonian niche concept. This concept defines a species' niche as a hypervolume with n–dimensional dimensions corresponding to environmental variables (Hutchinson 1957). The construction of climatic hypervolumes involved the application of multivariate kernel density estimation (Blonder et al. 2014). A Principal Component Analysis (PCA) was conducted based on 19 Bioclimatic variables (Karger et al. 2017), and the first two axes, which explained 70% of the total variance, were selected to calculate hypervolumes for each species–level lineage. The boundaries of kernel density estimates were delineated by the probability threshold, using the 0.85 quantile value. Hypervolume contours were plotted to project niche spaces, based on 5000 random background points, using the alphahull contour type and the alpha smoothing value 0.55. For ease of comprehension of the differential ordination of samples in the hyperspace, we employed box plots to visualize these differences. All analyses were performed in R studio v. 4.3.1 (RStudio Core Team 2023) using base functions and the packages hypervolume (Blonder et al. 2014) and alphahull (Pateiro–Lopez & Rodriguez–Casal 2016).

Results

In the present work, we describe the novel species *Trebouxia barrenoae*, providing a comprehensive and integrative study based on phylogenetic, morphological, physiological and ecological data which supports the delineation of this species.

Alignment description and phylogenetic analyses. The nrITS, rbcL and cox2 datasets included each 59 sequences, and had a length of 633, 789 and 441 bp, respectively. The number of variable sites (parsimony–informative sites in parentheses) in the corresponding alignments were 177 (128), 56 (43), and 86 (73). ML phylogenetic tree analyses in RAxML based on nrITS, rbcL and cox2 data estimated topologies with a final LogLikelihood of –2499.4562, –1484.5533 and –1128.1969, respectively. MrBayes analyses reached an ASDSF value of 0.005 after 1.62×10^6, 1.99×10^6 and 4.74×10^6 generations, respectively, and Estimated Sample Sizes (EESs) were well above 200 for all parameters in all three phylogenies. Because ML and MrBayes topologies showed no supported conflicts, the nrITS topology inferred with MrBayes is presented in Figure 1 (see Supplementary Fig. S1 and S2 for cox2 and rbcL phylogenies). The nrITS phylogeny, revealed the type specimen of the new *Trebouxia* species (collection ASUV143, see Taxonomy section below) forming a monophyletic clade together with four specimens formerly assigned to *Trebouxia* sp. S02 (KR914065, KJ623941, KJ623945 and KJ623946) with a BS support of 72% (PP = 0.95). The number of nucleotide differences in the barcode nrITS region of the specimen representing the newly described species and these four sequences was two or less. Due to the polytomy observed within the undescribed species *Trebouxia* sp. S02, the sister species of *Trebouxia barrenoae* sp. nov. is not resolved. Another specimen of *Trebouxia* sp. S02_S08 (KJ623944) from a thallus of *Lasallia pustulata* (L.) Mérat collected in Greece (Sadowska–Deś et al. 2014) was revealed as close species of the new *Trebouxia* species, but it differed in seven bp from the new species' nrITS sequence. At a greater scale, the new species and its sister lineage were placed in a clade including other specimens originally assigned to *Trebouxia* sp. S02. Our phylogeny showed that the undescribed *Trebouxia* sp. S02, as originally delimited (Leavitt et al. 2015), is polyphyletic, which agrees with results of Muggia et al. (2020). Finally, the other formally described species in *Trebouxia* clade S (*T. angustilobata*, *T. simplex* and *T. suecica*), which were well resolved in this phylogeny, were not shown to be close relatives of the new species. The resolution provided by the nrITS phylogeny was lost with rbcL and cox2 (Supplementary Fig. S1 and S2). The alignments of these two markers were very homogeneous and did not show variability among the sequences, with a maximum of five nucleotides. In addition, rbcL and cox2 did not provide enough information to resolve the clades of the formal species included in this clade, especially *T. angustilobata* and *T. suecica*.

Morphological and ultrastructural description of *Trebouxia barrenoae* sp. nov. in culture and in symbiosis. Mature cells were characterized by a regular spherical shape with a diameter ranging from 9 to 17 µm (Figs 2A, G–K), and showed a single central chloroplast that nearly occupied the whole volume of the cytoplasm and displayed shallow, elongated lobes (Fig. 2G–K), recalling the 'shallowly lobed' type (Bordenave et al. 2022). TEM analyses corroborated the presence of an impressa–type pyrenoid that laid in the center of the cell (Fig. 2C); occasionally, secondary smaller pyrenoids scattered along the matrix co–existed with the central one (Fig. 2A). Pyrenoglobules were always present in moderate numbers arranged in a row adjacent to the invaginations of the tubules (Fig. 2A, C). The cell wall was composed of two layers (Fig. 2D, F). Asexual reproduction via autospores was observed; irregularly shaped autosporangia (12–19 µm) usually contained 4–16 autospores, tightly appressed to each other (Fig. 2I, K). Zoospores were not observed, and sexual reproduction was not observed.

In symbiosis**,** this microalga displayed slight morphological variations (Supplementary Fig. S3), as thylakoid membranes of the chloroplast were laxer than in culture. The interactions between phycobiont cells and fungal hyphae in the observed thalli were interpreted as type–1 intraparietal haustoria (Honegger 1986).

Climatic distribution of *Trebouxia barrenoae* sp. nov. Two–dimensional hypervolumes were constructed for *T. barrenoae* sp. nov. and the other three described species in *Trebouxia* clade S: *T. angustilobata*, *T. simplex* and *T. suecica* (Fig. 3). The climatic hypervolume for all species overlapped in a substantial area that corresponded to the temperate forest of northern Europe, which is characterized by cold winters and relatively warm summers (Dreiss & Volin 2020). Consequently, all phycobionts showed relatively high temperature seasonality levels (BIO4, Fig. 3C). Nevertheless, each species showcased an intricate expansion of its ecological niche into diverse climatic regions. The new species *T. barrenoae* sp. nov, which predominantly occupied humid and relatively cold areas (BIO11, 17, 18, Figure 3D, E), exhibited the narrowest hypervolume, compared to the remaining three *Trebouxia*. In contrast, *T. suecica* spanned the entire Y–axis gradient and revealed its preference for warmer locations. *Trebouxia simplex* also exhibited a broader acceptance range across diverse climatic types, unraveling two isolated zones: the first one overlapped with *T. angustilobata* and represented areas with colder and drier climates; the second represented locations with very high isothermatility (e.g., Costa Rica).

Taxonomy
Class *Trebouxiophyceae*
Order *Trebouxiales*
Family *Trebouxiaceae* Friedl
Genus *Trebouxia* Puymaly

***Trebouxia barrenoae* sp. nov. Pazos, Chiva, Garrido–Benavent et Moya**
Description: Vegetative mature cells spherical, 9–17 µm wide. Cell wall composed by two layers, with the inner one being thicker than the outer one. Nucleus

Fottea, Olomouc, 25(1): 68–80, 2025
DOI: 10.5507/fot.2024.010

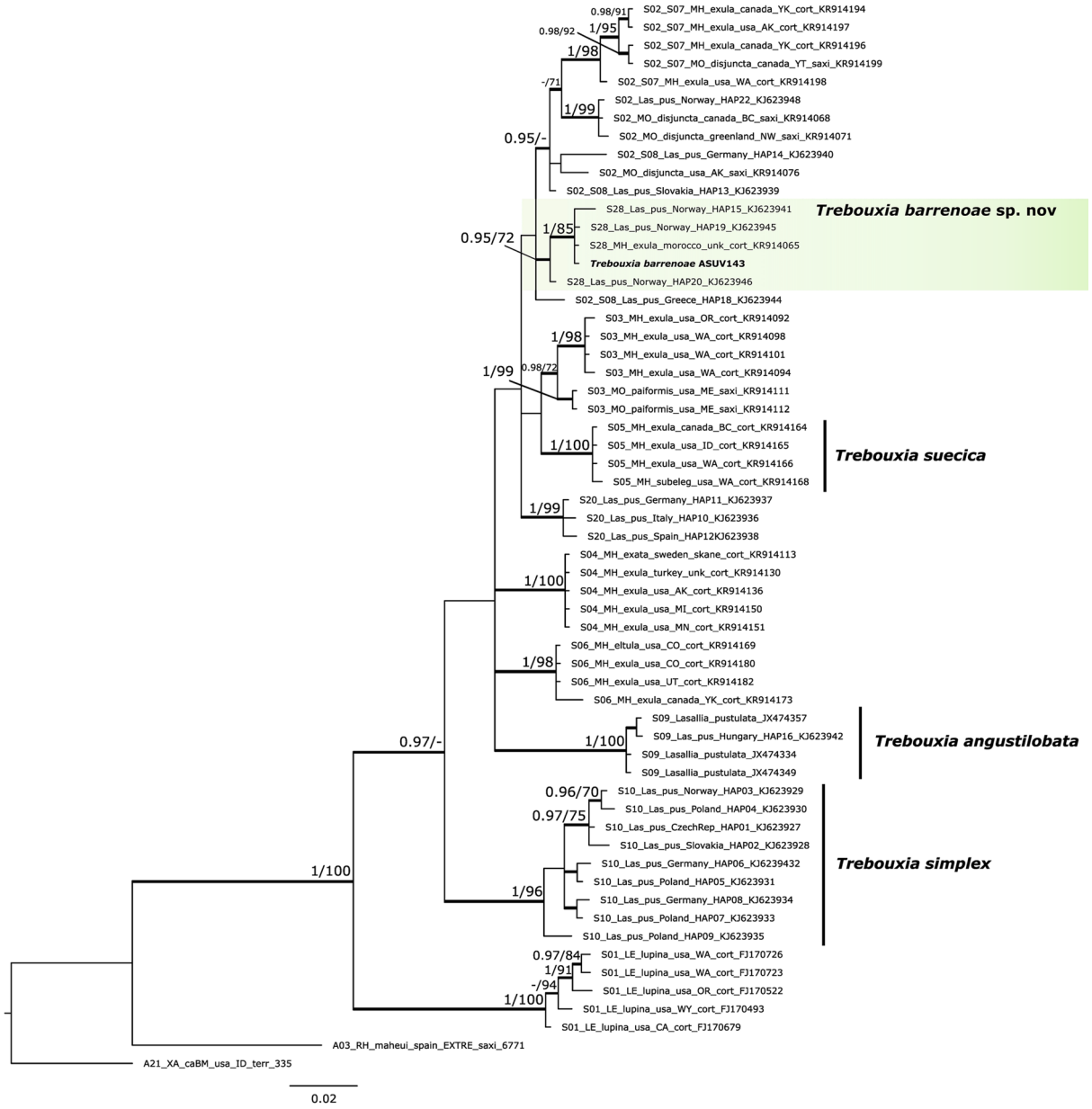

Fig. 1. MrBayes phylogram constructed using the nrITS dataset that depicts evolutionary relationships among described and still undescribed *Trebouxia* species–level lineages in clade S. Each tip indicates the species code of each *Trebouxia* clade following Muggia et al. (2020). The new species *Trebouxia barrenoae* sp. nov. is highlighted in a green box. Thickened branches indicate bootstrap support (BS, RAxML) ≥ 70% and/or posterior probabilities (PP, MrBayes) ≥ 0.95.

marginal, between the chloroplast lobes. Chloroplast central, shallowly lobed, with elongated lobes meandering around the chloroplast surface. A large central, impressa–type pyrenoid and several satellite smaller ones scattered throughout the chloroplast. Pyrenoids with radial, unbranched tubules penetrating a thick matrix; pyrenoglobules found in moderate numbers in the pyrenoid matrix, arranged linearly adjacent to the pyrenotubules. Asexual reproduction consisting in the formation of 4–16 autospores within irregularly shaped, 12–19 µm wide autosporangia. Zoospores not observed. Sexual reproduction not observed (Table 1).

Holotype: Dried material number VAL_Algae 3072 deposited at the VAL Herbarium (VAL_Algae Collection) of Valencia.

Iconotype (designated here to support the holotype): Fig. 2.

Type locality: Europe, Spain, Comunitat Valenciana, Castelló, El Toro, Puntal de los Peiros, 39°57’32.3”N, 0°46’35.5”W, 30SXK8925, alt. 1150 m, low supramediterranean (ITC0203) – low subhumid (IO = 4.7) bioclimate, as lichenized partner of the mycobiont *Pseudevernia furfuracea*, collected on *Pinus sylvestris*, 17 May 2022, leg. S. Chiva and P. Moya.

Etymology: The species is named after Prof. Dr. Eva Barreno, a renowned Spanish lichenologist whose studies

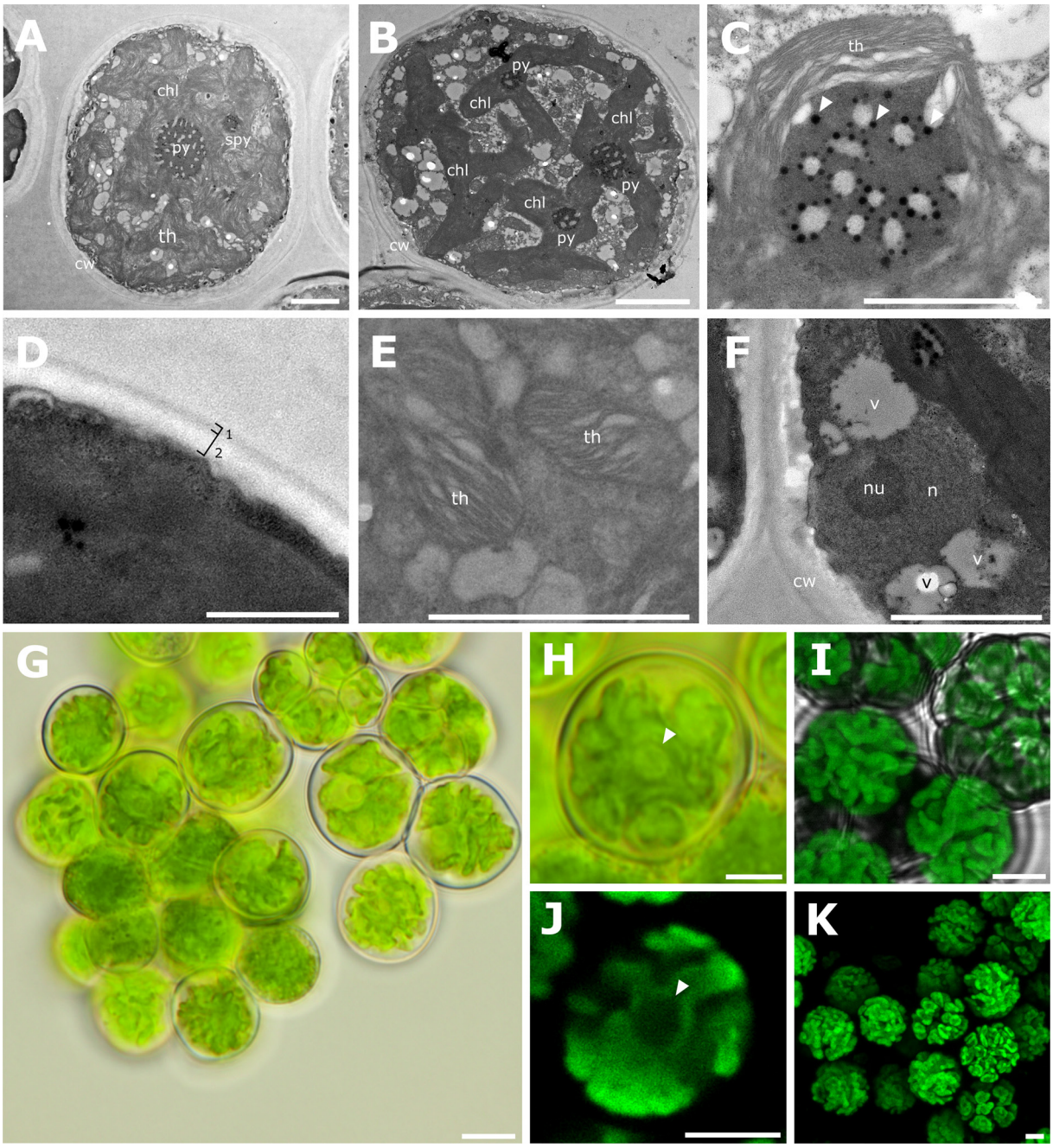

Fig. 2. Morphology of *Trebouxia barrenoae* sp. nov. (reference strain: ASUV143) by TEM (A–F), LM (G, H) and CSLM (I–K): (A) ultrastructure of *T. barrenoae* in culture; (B) mature cell with several chloroplasts before cytokinesis to form an autosporangium; (C) detail of the impressa–type pyrenoid, white arrows indicate pyrenoglobules; (D) detail of the cell wall containing two layers; (E) detail of the thylakoids of the chloroplast; (F) detail of the nucleus; (G) gross morphology of vegetative cells and autosporangia; (H) morphology of a mature cell, white arrow indicates the pyrenoid; (I) confocal reconstruction of the morphology of autosporangia, immature cells undergoing first chloroplast division and mature cells; (J) morphology of a mature cell and detail of the pyrenoid by CSLM; (K) gross morphology of vegetative cells and autosporangia with cells undergoing first chloroplast division by CLSM. Abbreviations: (chl) chloroplast, (cw) cell wall, (n) nucleus, (nu) nucleolus, (py) pyrenoid, (spy) satellite pyrenoid, (th) thylakoids and (v) vesicles. Scale bars 2 μm (A–F), 5 μm (G–K).

have significantly contributed to the understanding of mutualistic interactions in lichens.

Ecology and distribution: This new lichenized microalga predominantly distributes in temperate forests across the Northern Hemisphere (Fig. 3A), especially in Europe, with occurrences that extend beyond the European continent to include North America (Canada), Africa (Morocco), and Asia (Iran; see Supplementary Table S4). This microalga associates primarily with lichenized fungi of the family *Parmeliaceae*, but also with members of other families, such as *Caliciaceae*, *Lecanoraceae*, *Ochrolechiaceae*, *Psoraceae*, *Teloschistaceae*, and *Umbilicariaceae*. Finally, *Trebouxia barrenoae* sp. nov. mostly thrives on epiphytic lichens growing on *Picea* and *Pinus* spp., both phorophytes characterized by their acidic bark. Additionally, it has been found to a lesser

Fottea, Olomouc, 25(1): 68–80, 2025
DOI: 10.5507/fot.2024.010

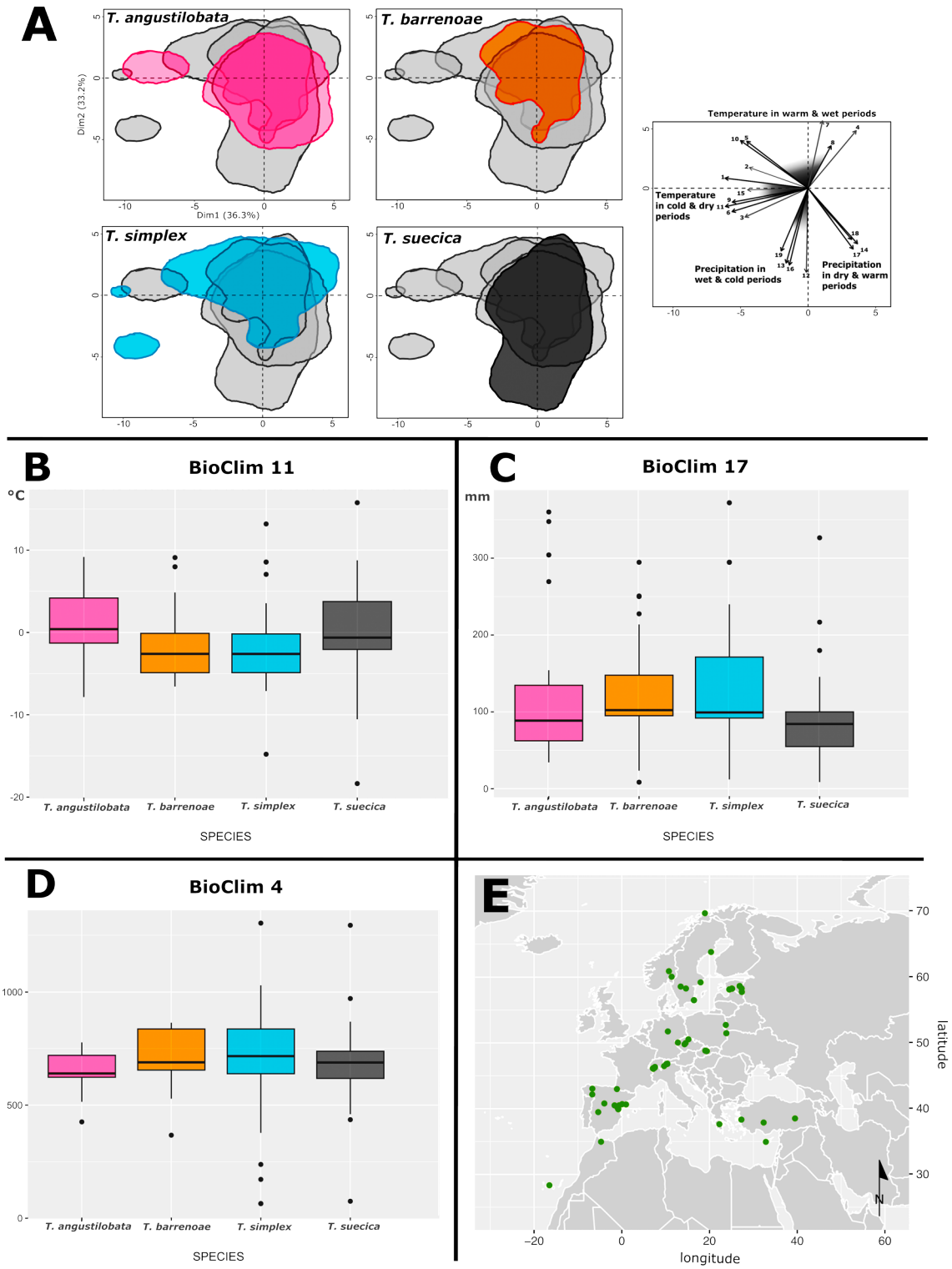

Fig. 3. Biogeography and climatic niche of *Trebouxia barrenoae* sp. nov.: (A) climatic niche hypervolumes for *T. barrenoae*, *T. angustilobata*, *T. simplex* and *T. suecica* based on climatic PC1–PC2 axes; BioClim variables: 1 = annual mean temperature (ºC), 2 = mean diurnal range (ºC), 3 = isothermality (adimensional, index), 4 = temperature seasonality (adimensional, standard deviation), 5 = max temperature of warmest month (ºC), 6 = min temperature of coldest month (ºC), 7 = temperature annual range (ºC), 8 = mean temperature of wettest quarter (ºC), 9 = mean temperature of driest quarter (ºC), 10 = mean temperature of warmest quarter (ºC), 11 = mean temperature of coldest quarter (ºC), 12 = annual precipitation (mm), 13 = precipitation of wettest month (mm), 14 = precipitation of driest month (mm), 15 = precipitation seasonality (adimensional, coefficient variation), 16 = precipitation of wettest quarter (mm), 17 = precipitation of driest quarter (mm), 18 = precipitation of warmest quarter (mm), 19 = precipitation of coldest quarter (mm) (Karger et al. 2017); (B) box–plot diagram representing differences in BioClim 4: Temperature Seasonality (standard deviation *100); (C) box–plot diagram representing differences in BioClim 11: Mean Temperature of Coldest Quarter; (D) box–plot diagram representing differences in BIO17 = Precipitation of Driest Quarter; (E) Map showing the geographical distribution of *T. barrenoae* in Europe and the Canary islands.

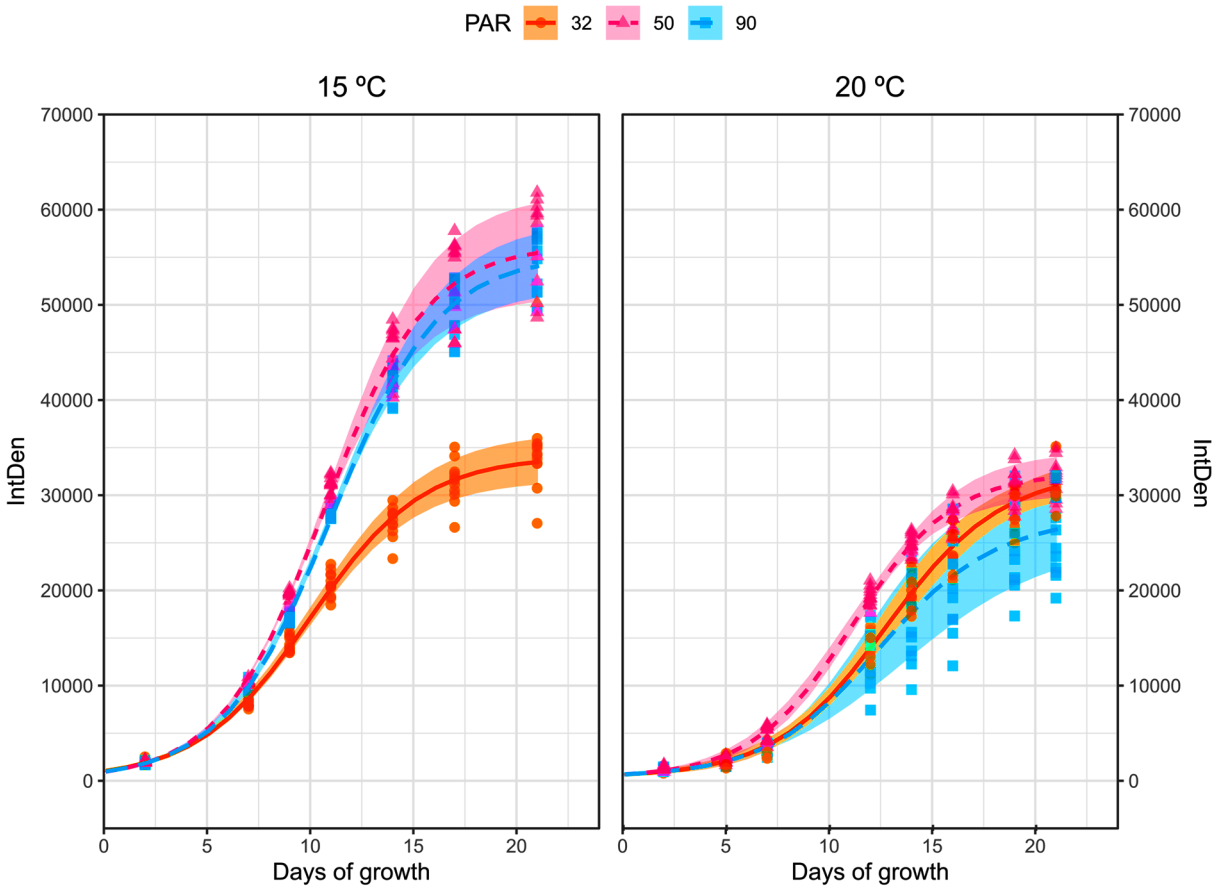

Fig. 4. Modelled growth curves of light radiation and temperature treatments. Lines represents average predicted value of models; shaded areas show standard deviation (s.d.) 95% confidence interval. Original data points are shown (n = 12). See Supplementary Figure S4 for mean ± s.d. of growth parameters.

extent in saxicolous and terricolous lichens.
Reference strains: ASUV143 and BEA2100B.
GenBank accession numbers: OK577856 (nrITS), PP327373 (*cox*2), PP327374 (rbcL) and PP626696 (LSU).
Phylogeny: *Trebouxia barrenoae* (S28) belongs to *Trebouxia* clade S and is close to *Trebouxia* sp. S02 according to the nrITS phylogeny reconstructed under ML and BI (Fig. 1).
Physiological features: Colonies of *Trebouxia barrenoae* sp. nov. were bigger (κ) and showed higher maximum growth rates (μ_m) when grown at 15 °C than at 20 °C at all light intensities except for 32 PAR (Fig. 4), the lower that was tested (Supplementary Fig. S4). These results agree with the photosynthetic efficiency F_v/F_m (Supplementary Fig. S5) which is higher for all light intensities at 15 °C than at 20 °C.
Differential diagnosis: The new species reported here displays slightly less flattened chloroplast lobes than its counterparts of *Trebouxia* clade S. It differs from *T. australis* and *T. simplex* by its reduced number of pyrenoglobules, which are neatly aligned around the pyrenotubules. *Trebouxia australis* and *T. simplex* exhibit a less organized pyrenoglobule distribution in the pyrenoids, being dispersed throughout the matrix (Table 1). Furthermore, the new species clearly diverges molecularly from other *Trebouxia* clade S lineages in the nrITS, rbcL, LSU and cox2 nucleotide sequences.

Discussion

The new species *T. barrenoae* sp. nov. belongs to *Trebouxia* clade S, whose species have been progressively delineated since the seminal work of Leavitt et al. (2015), followed by a latter study by Muggia et al. (2020). Nevertheless, this *Trebouxia* clade harbors numerous undescribed species, surpassing those already taxonomically described. Our study not only contributes to the refinement of the taxonomic and systematic understanding within this group, but also addresses the ongoing need to increase our knowledge regarding its ecology, physiology and evolutionary relationships. Concerning *Trebouxia* sp. S02, we corroborated previous phylogenetic analyses published by Muggia et al. (2020), which elucidated the polyphyletic nature of this lineage; consequently, the taxonomic landscape of this clade is improved with the description of *T. barrenoae* sp. nov. However, significant taxonomic work employing integrative methodologies, which consider not only phylogenetic relationships but also ecological and physiological traits, is essential to

Fottea, Olomouc, 25(1): 68–80, 2025
DOI: 10.5507/fot.2024.010

Table 1. Morphological comparison among *Trebouxia* clade S species. Asterisks indicate descriptions derived from the species' protologue. The newly described *Trebouxia* is highlighted in bold.

***Trebouxia* spp.**	**Shape and size**	**Chloroplast type**	**Pyrenoid type**	**Reproduction**
T. angustilobata A. Beck	Spherical, (5−)7−22 µm cell diameter (Beck 2002) *	Central, narrow lobed (Beck 2002) *	Radial pattern, similar to impressa–type (Beck 2002) *	Forming autospores, zoospores and aplanospores. Zoospores oval, 3−4 × 6−8 µm (Beck 2002) *
T. australis A. Beck	Spherical, (5−)7−23 (very rarely up to 25) µm cell diameter (Beck 2002) *	Narrow lobed (Beck 2002) * Central, shallowly lobed, with narrow lobes (Bordenave et al. 2022)	Multiple impressa–type, pyrenoglobules scattered throughout the matrix (Bordenave et al. 2022)	Forming zoospores, aplanospores and autospores. Zoospores oval, 3−4 × 6−8 µm. (Beck 2002) *
T. barrenoae	**Spherical, 9−17 µm cell diameter**	**Central, shallowly lobed, elongated lobes**	**Multiple impressa–type, pyrenoglobules aligned around the tubules**	**Forming autospores. Zoospores and aplanospores not observed.**
T. brindabellae A. Beck	Spherical, (5−)7−25 µm cell diameter (Beck 2002) *	Type not reported, central, with long, broad lobes (Beck 2002) *	Radial pattern, similar to impressa–type (Beck 2002) *	Forming autospores, zoospores and aplanospores (Beck 2002) *
T. simplex Tschermak–Woess	Spherical, (14−)16−23 µm cell diameter (Tschermak–Woess 1978) *	Central, shallowly and deeply lobed, with long, broad lobes that usually appear twisted (Tschermak–Woess 1978*, Bordenave et al. 2022)	Multiple impressa–type, pyrenoglobules scattered throughout the matrix (Bordenave et al. 2022)	Forming zoospores, aplanospores and autospores (4–32). Zoospores oval, 3−4 × 6−8 µm (Tschermak–Woess 1978) *
T. suecica A. Beck	Spherical, (5−)7−13 (rarely up to 15) µm cell diameter (Beck 2002) *	Type not reported, central, deeply lobed, with broad lobes, which usually appear twisted (Beck 2002) *	Radial pattern, similar to impressa–type (Beck 2002) *	Forming zoospores, aplanospores and autospores. (Beck 2002) *

address taxa delimitation in other clades comprising the original *Trebouxia* sp. S02.

Recently, Muggia *et al*. (2020) reappraised species diversity and evolutionary relationships and generated a multi–locus phylogenetic reference framework on which to base future research in *Trebouxia* systematics and taxonomy. In the present study, the combined use of nrITS, rbcL, and cox2 for multi–locus tree inference was conducted (data not shown). However, we found that separate and concatenated datasets yielded incongruent phylogenetic results; in fact, the multi–locus approach led to the loss of clade resolution provided by nrITS alone, given that rbcL and cox2 were not as resolutive as the barcode marker. In fact, these two protein–coding loci failed to distinguish the three already formally described species within this clade in single–locus phylogenies. The most likely explanation to our findings is incomplete lineage sorting, perhaps because the studied *Trebouxia* group evolved at shallow time depths (Maddison & Knowles 2006). This phenomenon has been reported frequently in lichenized fungi (e.g., Zhao et al. 2017; Boluda et al. 2021). All in all, our study highlights the strength of the highly variable nrITS for species delimitation in complex *Trebouxia* groups and the unsuitability of using rbcL and cox2 in multi–locus phylogenies, at least for our target *Trebouxia* clade S. We therefore emphasize the importance of verifying the phylogenetic resolution of individual markers before concatenation, the need to continue searching for markers to straightforward species delimitation in *Trebouxia* and, finally, the importance of incorporating morphological and ecological data to support molecular information. The new taxon *Trebouxia barrenoae* sp. nov. was found almost exclusively in the eastern Iberian Peninsula in association with two parmeliod asexually reproducing lichens: *Parmelia serrana* and *Pseudevernia furfuracea*. To a lesser extent, Pazos et al. (submitted) identified *T. barrenoae* sp. nov. as phycobiont of the sexually reproducing species *Xanthoria parietina* and *Anaptychia ciliaris*. In accordance with these data, metadata associated to GenBank sequences from Eurasian lichens reported this species to be in association preferably with asexually–reproducing lichens of the family *Parmeliaceae*, such as species in *Bryoria* (Ruprecht et al. 2014; Boluda et al. 2021), *Cetraria* (Bačkor et al. 2010; Domaschke et al. 2013; Onuț–Brännström et al. 2018), *Hypogymnia* (Bhattacharya et al. 1996; Singh et al. 2019; Mark et al. 2020), *Melanohalea* (Leavitt et al. 2015), *Montanelia* (Peksa et al. 2022), *Foveolaria* (Opanowicz & Grube 2004), *Parmelia* (Singh et al. 2019; Moya et al. 2021; Ossowska et al. 2019; Bordenave et

al. 2022; Peksa et al. 2022) and *Pseudevernia* (Kroken & Taylor 2000; Singh et al. 2019; Mark et al. 2020; Peksa et al. 2022). Other mainly asexual lichens such as *Ochrolechia bahusiensis* H. Magn. (Singh et al. 2019) and *Lasallia pustulata* (L.) Mérat (Sadowska–Deś et al. 2014) were found in association with this microalga. In the American continent, *T. barrenoae* sp. nov. was found to be the phycobiont of *Evernia mesomorpha* Nyl. in Canada (Piercey–Normore 2009). Moreover, GenBank documented its minor presence in thalli from diverse sexually reproducing lichens (i.e., *Buellia elegans* Poelt (Ruprecht et al. 2014), *Lecanora cenisia* Ach. (Peksa et al. 2022) and *Psora decipiens* (Hedw.) Hoffm. (Ruprecht et al. 2014)). These results suggest a notable preference of *T. barrenoae* sp. nov. for the association with asexually reproducing lichens.

A recent study by Peksa et al. (2022) analyzed how substrate can influence myco– and phycobiont association patterns in rocky lichen communities and found a substantial preference of *Trebouxia* clade S for acidic substrates. In a previous study, Beck (2002) elucidated that *T. simplex* (clade S) is a common photobiont in lichens growing on acid and heavy metal rich rocky substrates. Our results are in alignment with previous studies and reported the preference of *T. barrenoae* sp. nov. for acidic substrates, particularly favoring lichens inhabiting barks of *Pinus* spp. in the Iberian Peninsula and *Picea* spp. in the rest of Europe, both characteristic by showing an acidic pH (see Supplementary Table S4). These results reinforce the pronounced specificity exhibited by species within *Trebouxia* clade S towards acidic substrates, and document for the first time its choice for epiphytic habitats. Further investigations should conduct physiological analyses to elucidate the growth rate of these microalgae across varying pH gradients.

Our results revealed the predominance of the newly described species *T. barrenoae* sp. nov. in areas characterized by high humidity levels and relatively cold conditions, and physiological analyses corroborated its preferential growth affinity towards low temperatures. Additionally, metadata associated with *Trebouxia* sequences deposited in GenBank (Supplementary Table S4) allowed us to delimit the geographic distribution of this species, which appears widespread in the northern Hemisphere, especially in Mediterranean and temperate regions of Eurasia. Furthermore, our climatic niche analyses among *Trebouxia* clade S species revealed an overlapping hypervolume, indicative of shared ecological preferences among them. It has been previously reported that *Trebouxia* lineages within clade S occur in cold regions characterized by dry climates in the northern Hemisphere (Garrido–Benavent et al. 2020, De Carolis et al. 2022, Nelsen et al. 2021, 2022). Furthermore, Kosecka et al. (2022) revealed *Trebouxia* clade S selection for habitats located in altitudes above 1943 m a.s.l. Our data supports this idea as the presence of *T. barrenoae* sp. nov. has been reported in lichens growing above 1200 m a.s.l., at least in southern Europe. Moreover, light intensity analyses showed that this species exhibits its optimal growth under higher PAR intensities (i.e., 50 and 90 PAR) than the standard 32 PAR for symbiotic microalgae (Casano et al. 2010), which appear at higher altitude levels and open areas (e.g., reduced pollution regions) (Sahu et al. 2019; García–Rodríguez et al. 2021; Proutsos et al. 2022).

In conclusion, the description of *T. barrenoae* sp. nov. expands the formally recognized diversity of the genus *Trebouxia* to 32 taxonomically described species and holds deep implications for biodiversity studies within forest ecosystems, offering a more comprehensive understanding of lichen symbioses. By providing a refined taxonomic framework, our findings are poised to enhance communication and facilitate more nuanced approaches to conservation policies.

Acknowledgements

This study was supported by Generalitat Valenciana (GVA, excellence in research: PROMETEO/2021/005 to E. Barreno and P. Carrasco) and the Ministerio de Ciencia e Innovación of the Spanish Government (PID2021–127087NB–I00 to I. Garrido–Benavent and P. Carrasco). S.C. received funding from a postdoctoral grant: Margarita Salas of the Ministerio de Universidades—Spain (Next generation EU, MS21–058). C.D.B. received funding from a postdoctoral contract María Zambrano of Ministerio de Universidades, Next Generation UE (grant ZA21–046). A.G. received funding from a postdoctoral contract of Generalitat Valenciana and European Social Fund (APOSTD21). We would like to thank Lucie Vančurová (Czech Republic) for sharing the climatic niche script.

References

Archibald, P. A. (1975): *Trebouxia* Puymaly (*Chlorophyceae*, *Chlorococcales*) and *Pseudotrebouxia* gen. nov. (*Chlorophyceae*, *Chlorosarcinales*). – Phycologia 14 : 125–137.

Bačkor M.; Peksa O.; Škaloud P. & Bačkorová M. (2010): Photobiont diversity in lichens from metal–rich substrata based on ITS rDNA sequences. – Ecotoxicology and Environmental Safety 73: 603–12.

Barreno, E.; Muggia, L.; Chiva, S.; Molins, A.; Bordenave, C.; García–Breijo, F. & Moya, P. (2022): *Trebouxia lynnae* sp. nov. (former *Trebouxia* sp. TR9): biology and biogeography of an epitome lichen symbiotic microalga. – Biology 11: 1196.

Beck, A. (1999): Photobiont inventory of a lichen community growing on heavy–metal–rich rock. – The Lichenologist 31: 501–510.

Beck, A. (2002): Selektivität der Symbionten schwermetalltoleranter Flechten [PhD. thesis]. – 162 pp., Ludwig-Maximilians-Universität München, Munich, Germany.

Bhattacharya, D.; Friedl, T. & Damberger, S. (1996): Nuclear–encoded rDNA group I introns: origin and phylogenetic relationships of insertion site lineages in the green algae. – Molecular Biology and Evolution 13: 978–989.

Bischoff, H. W.; Bold, H. C. (1963): Physiological studies: IV. – In: Some soil algae from enchanted rock and related algal species. – 6318 pp., University of Texas, Austin, TX, USA.

Blonder, B.; Lamanna, C.; Violle, C. & Enquist, B. J.

Fottea, Olomouc, 25(1): 68–80, 2025
DOI: 10.5507/fot.2024.010

(2014): The n-dimensional hypervolume. – Global Ecology and Biogeography 23: 595–609.

Bold, H. C. (1949): The morphology of *Chlamydomonas chlamydogama*, sp. nov. –Bulletin of the Torrey Botanical Club 76: 101–108.

Boluda, C. G.; Rico, V. J.; Naciri, Y.; Hawksworth, D. L. & Scheidegger, C. (2021): Phylogeographic reconstructions can be biased by ancestral shared alleles: The case of the polymorphic lichen *Bryoria fuscescens* in Europe and North Africa. – Molecular Ecology 30: 4845–4865.

Bordenave, C. D.; Muggia, L.; Chiva, S.; Leavitt, S. D.; Carrasco, P. & Barreno, E. (2022): Chloroplast morphology and pyrenoid ultrastructural analyses reappraise the diversity of the lichen phycobiont genus *Trebouxia* (*Chlorophyta*). – Algal Research 61: 102561.

Casano, L. M.; del Campo, E. M.; García-Breijo, F. J.; Reig-Armiñana, J.; Gasulla, F.; Del Hoyo, A.; Guéra, A. & Barreno, E. (2011): Two *Trebouxia* algae with different physiological performances are ever-present in lichen thalli of *Ramalina farinacea.* Coexistence versus competition? – Environmental Microbiology 13: 806–818.

Chiva, S.; Dumitru, C.; Bordenave, C. D. & Barreno, E. (2021): *Watanabea* green microalgae (*Trebouxiophyceae*) inhabiting lichen holobiomes: *Watanabea lichenicola* sp. nova. – Phycological Research 69: 226–236.

De Carolis, R.; Cometto, A.; Moya, P.; Barreno, E.; Grube, M.; Tretiach, M.; Leavitt, S. D. & Muggia, L. (2022): Photobiont diversity in lichen symbioses from extreme environments. – Frontiers in Microbiology 13: 809804.

Del Campo, E. M.; Casano, L. M.; Gasulla, F. & Barreno, E. (2010): Suitability of chloroplast LSU rDNA and its diverse group I introns for species recognition and phylogenetic analyses of lichen–forming *Trebouxia* algae. – Molecular Phylogenetics and Evolution 54: 437– 444.

Domaschke, S.; Vivas, M.; Sancho, L. G. & Printzen, C. (2013): Ecophysiology and genetic structure of polar versus temperate populations of the lichen *Cetraria aculeata*. – Oecologia 173: 699–709.

Ettl, H. & Gärtner, G. (2014): Syllabus der Boden–, Luft– und Flechtenalgen. – 773 pp., Springer, Berlin/ Heidelberg, Germany.

Friedl, T. (1989): Systematik und Biologie von Trebouxia (Microthamniales, Chlorophyta) als Phycobiont der Parmeliaceae (lichenisierte Ascomyceten) [PhD thesis]. – 218 pp., Fakultät für Biologie, Chemie und Geowissenschaften, Universität Bayreuth, Bayreuth, Germany.

García–Rodríguez, A.; Granados–López, D.; García–Rodríguez, S.; Díez–Mediavilla, M. & Alonso–Tristán, C. (2021): Modelling Photosynthetic Active Radiation (PAR) through meteorological indices under all sky conditions. – Agricultural and Forest Meteorology 310: 108627.

Garrido–Benavent, I.; Chiva, S.; Bordenave, C. D.; Molins, A. & Barreno, E. (2022): *Trebouxia maresiae* sp. nov. (*Trebouxiophyceae*, *Chlorophyta*), a new lichenized species of microalga found in coastal environments. – Cryptogamie, Algologie 43: 135–145.

Garrido–Benavent, I.; Pérez–Ortega, S.; de los Ríos, A. & Fernández–Mendoza, F. (2020): Amphitropical variation of the algal partners of *Pseudephebe* (*Parmeliaceae*, lichenized fungi). – Symbiosis 82: 35–48.

Gartner, G. (1985): Die Gattung *Trebouxia* Puymaly (*Chlorellales*, *Chlorophyceae*). – Algological Studies 71: 495–548.

Gasulla, F.; Guéra, A. & Barreno, E. (2010): A simple and rapid method for isolating lichen photobionts. – Symbiosis 51: 175–179.

Grube, M. (2024): Lichens. – In: Fungal Associations; Cham. – pp. 145–179, Springer International Publishing.

Guiry, M. D.; Guiry, G. M. AlgaeBase, World–Wide Electronic Publication. – National University of Ireland: Galway, Ireland, 2019; Available at https://www.algaebase.org (accessed on 22 January 2024).

Helms, G.; Friedl, T.; Rambold, G. & Mayrhofer, H. (2001): Identification of photobionts from the lichen family *Physciaceae* using algal–specific ITS rDNA sequencing. – The Lichenologist 33: 73–86.

Honegger, R. (1986): Ultrastructural studies in lichens: II. Mycobiont and photobiont cell wall surface layers and adhering crystalline lichen products in four *Parmeliaceae*. – New Phytologist 103: 797–808.

Hutchinson, G. E. (1957): Concluding remarks. – Cold Spring Harbor Symposia on Quantitative Biology 22: 415–427.

Karger, D.N.; Conrad, O.; Böhner, J.; Kawohl, T.; Kreft, H.; Soria–Auza, R.W. & Kessler, M. (2017): Climatologies at high resolution for the earth's land surface areas. – Scientific Data 4: 1–20.

Katoh, K. & Standley, D. M. (2013): MAFFT multiple sequence alignment software version 7: improvements in performance and usability. – Molecular Biology and Evolution 30: 772–780.

Katoh, K.; Misawa, K.; Kuma, K. I. & Miyata, T. (2002): MAFFT: a novel method for rapid multiple sequence alignment based on fast Fourier transform. – Nucleic Acids Research 30: 3059–3066.

Kosecka, M.; Kukwa, M.; Jabłońska, A.; Flakus, A.; Rodriguez–Flakus, P.; Ptach, Ł. & Guzow–Krzemińska, B. (2022): Phylogeny and ecology of *Trebouxia* photobionts from Bolivian lichens. – Frontiers in Microbiology 13: 779–784.

Kroken, S. & Taylor, J. W. (2000): Phylogenetic species, reproductive mode, and specificity of the green alga *Trebouxia* forming lichens with the fungal genus *Letharia*. –Bryologist 103: 645–660.

Lanfear, R.; Calcott, B.; Ho, S. Y. & Guindon, S. (2012): PartitionFinder: combined selection of partitioning schemes and substitution models for phylogenetic analyses. – Molecular Biology and Evolution 29: 1695–1701.

Leavitt, S. D.; Kraichak, E.; Nelsen, M. P.; Altermann, S.; Divakar, P. K.; Alors, D.; Esslinger, T. L.; Crespo, A. & Lumbsch, T. (2015): Fungal specificity and selectivity for algae play a major role in determining lichen partnerships across diverse ecogeographic regions in the lichen-forming family *Parmeliaceae* (*Ascomycota*). – Molecular Ecology 24: 3779–3797.

Lindgren, H.; Velmala, S.; Högnabba, F.; Goward, T.; Holien, H. & Myllys, L. (2014): High fungal selectivity for algal symbionts in the genus *Bryoria*. – The Lichenologist 46: 681–695.

Maddison, W. P. & Knowles, L. L. (2006): Inferring phylogeny despite incomplete lineage sorting. – Systematic Biology 55: 21–30.

Mark, K.; Laanisto, L.; Bueno, C. G.; Niinemets, Ü.; Keller, C. & Scheidegger, C. (2020): Contrasting co-occurrence patterns of photobiont and cystobasidiomycete

yeast associated with common epiphytic lichen species. – New Phytologist 227: 1362–1375.

Mason–Gamer, R. J. & Kellogg, E. A. (1996): Testing for phylogenetic conflict among molecular data sets in the tribe *Triticeae* (*Gramineae*). – Systematic Biology 45: 524–545.

Miadlikowska, J.; Richardson, D.; Magain, N.; Ball, B.; Anderson, F.; Cameron, R.; Lendemer, J.; Truong, C. & Lutzoni, F. (2014): Phylogenetic placement, species delimitation, and cyanobiont identity of endangered aquatic *Peltigera* species (lichen-forming *Ascomycota*, *Lecanoromycetes*). – American Journal of Botany 101: 1141–1156.

Miller, M. A.; Pfeiffer, W. & Schwartz, T. (2010): Creating the CIPRES Science Gateway for inference of large phylogenetic trees. – In: Proceedings of the Gateway Computing Environments Workshop, New Orleans, LA, USA, 14 November 2010. – pp. 1–8, IEEE.

Molins, A.; Moya, P.; Garcia–Breijo, F. J.; José, R. A. & Barreno, E. (2018): A multi–tool approach to assess microalgal diversity in lichens: isolation, Sanger sequencing, HTS and ultrastructural correlations. – The Lichenologist 50: 123–138.

Moya, P.; Chiva, S.; Catalá, M.; Garmendia, A.; Casale, M.; Gomez, J.; Pazos, T.; Giordani, P.; Calatayud, V. & Barreno, E. (2023). Lichen biodiversity and near–infrared metabolomic fingerprint as diagnostic and prognostic complementary tools for biomonitoring: a case study in the eastern Iberian Peninsula. – Journal of Fungi 9: 1064.

Moya, P.; Molins, A.; Škaloud, P.; Divakar, P. K.; Chiva, S.; Dumitru, C.; Molina, M. C.; Crespo, A. & Barreno, E. (2021): Biodiversity patterns and ecological preferences of the photobionts associated with the lichen–forming genus *Parmelia*. – Frontiers in Microbiology 12: 765310.

Muggia, L.; Leavitt, S. & Barreno, E. (2018): The hidden diversity of lichenized *Trebouxiophyceae* (*Chlorophyta*). – Phycologia 57: 503–524.

Muggia, L.; Nelsen, M. P.; Kirika, P. M.; Barreno, E.; Beck, A.; Lindgren, H.; Lumbsch, H. T.; Leavitt, S. D. & Trebouxia Working Group. (2020): Formally described species woefully underrepresent phylogenetic diversity in the common lichen photobiont genus *Trebouxia* (*Trebouxiophyceae*, *Chlorophyta*): an impetus for developing an integrated taxonomy. – Molecular Phylogenetics and Evolution 149: 106821.

Nelsen, M. P.; Leavitt, S. D.; Heller, K.; Muggia, L. & Lumbsch, H. T. (2021): Macroecological diversification and convergence in a clade of keystone symbionts. – FEMS Microbiology Ecology 97: fiab072.

Nelsen, M. P.; Leavitt, S. D.; Heller, K.; Muggia, L. & Lumbsch, H. T. (2022): Contrasting patterns of climatic niche divergence in *Trebouxia*—a clade of lichen–forming algae. – Frontiers in Microbiology 13: 791546.

Nelsen, M. P.; Lücking, R.; Mbatchou, J. S.; Andrew, C. J.; Spielmann, A. A. & Lumbsch, H. T. (2011): New insights into relationships of lichen–forming *Dothideomycetes*. – Fungal Diversity 51: 155–162.

Onuț–Brännström, I.; Benjamin, M.; Scofield, D. G.; Heiðmarsson, S.; Andersson, M. G.; Lindström, E. S. & Johannesson, H. (2018): Sharing of photobionts in sympatric populations of *Thamnolia* and *Cetraria* lichens: evidence from high–throughput sequencing. – Scientific Reports 8: 4406.

Opanowicz, M. & Grube, M. (2004): Photobiont genetic variation in *Flavocetraria nivalis* from Poland (*Parmeliaceae*, lichenized *Ascomycota*). – The Lichenologist 36: 125–131.

Ossowska, E.; Guzow–Krzemińska, B.; Kolanowska, M.; Szczepańska, K. & Kukwa, M. (2019): Morphology and secondary chemistry in species recognition of *Parmelia omphalodes* group–evidence from molecular data with notes on the ecological niche modelling and genetic variability of photobionts. – MycoKeys 61: 39.

Pateiro–Lopez, B. & Rodriguez–Casal, A. (2016). Alphahull: generalization of the convex hull of a sample of points in the plane. – Available at: https:// cran.r–project.org/package=alphahull (Accessed 17 March, 2024).

Peksa, O.; Gebouská, T.; Škvorová, Z.; Vančurová, L. & Škaloud, P. (2022): The guilds in green algal lichens—An insight into the life of terrestrial symbiotic communities. – FEMS Microbiology Ecology 98: fiac008.

Piercey–Normore, M. D. (2009): Vegetatively reproducing fungi in three genera of the *Parmeliaceae* share divergent algal partners. – The Bryologist 112: 773–785.

Piercey-Normore, M. D. & DePriest, P. T. (2001): Algal switching among lichen symbioses. – American Journal of Botany 88: 1490–1498.

Proutsos, N.; Alexandris, S.; Liakatas, A.; Nastos, P. & Tsiros, I. X. (2022): PAR and UVA composition of global solar radiation at a high altitude Mediterranean forest site. – Atmospheric Research 269: 106039.

R Core Team. (2021): R: a language and environment for statistical computing. – Available online: https://www.R–project.org/ (accessed on 17 February 2024).

Rachoski, M.; Gazquez, A.; Calzadilla, P.; Bezus, R.; Rodriguez, A.; Ruiz, O.; Bernardina, A. & Maiale, S. (2015): Chlorophyll fluorescence and lipid peroxidation changes in rice somaclonal lines subjected to salt stress. – Acta Physiologiae Plantarum 37: 1–12.

Rambold, G.; Friedl, T. & Beck, A. (1998): Photobionts in lichens: possible indicators of phylogenetic relationships. – The Bryologist 101: 392–397.

Rivas–Martínez, S.; Penas, Á.; del Río, S.; Díaz González, T. E. & Rivas–Sáenz, S. (2017): Bioclimatology of the Iberian Peninsula and the Balearic Islands. – In: Loidi, J. (ed.): The vegetation of the Iberian Peninsula. – pp. 29–80, Springer, Cham, Switzerland.

Ronquist, F.; Teslenko, M.; Van Der Mark, P.; Ayres, D. L.; Darling, A.; Höhna, S.; Larget, B.; Liu, L.; Suchard, M. A. & Huelsenbeck, J. P. (2012): MrBayes 3.2: efficient Bayesian phylogenetic inference and model choice across a large model space. – Systematic Biology 61: 539–542.

RStudio Team. RStudio: Integrated Development Environment for R; RStudio, PBC: Boston, MA, USA, 2023. – Available online: https://www.algaebase.org (accessed on 17 January 2024).

Ruprecht, U.; Brunauer, G. & Türk, R. (2014): High photobiont diversity in the common European soil crust lichen *Psora decipiens.* – Biodiversity and conservation 23: 1771–1785.

Sadowska–Deś, A. D.; Dal Grande, F.; Lumbsch, H. T.; Beck, A.; Otte, J.; Hur, J. S.; Kim, J. & Schmitt, I. (2014): Integrating coalescent and phylogenetic approaches to delimit species in the lichen photobiont *Trebouxia*. – Molecular Phylogenetics and Evolution 76: 202–210.

Sahu, N.; Singh, S. N.; Singh, P.; Mishra, S.; Karakoti, N.; Bajpai, R.; Behera, S. K.; Nayaka, S. & Upreti, D. K.

Fottea, Olomouc, 25(1): 68–80, 2025
DOI: 10.5507/fot.2024.010

(2019): Microclimatic variations and their effects on photosynthetic efficiencies and lichen species distribution along elevational gradients in Garhwal Himalayas. – Biodiversity and Conservation 28: 1953–1976.

Schindelin, J.; Arganda–Carreras, I.; Frise, E.; Kaynig, V.; Longair, M.; Pietzsch, T.; Preibisch, S.; Rueden, C.; Saalfeld, S.; Schmid, B.; Tinevez, J.; White, D. J.; Hartenstein, V.; Eliceiri, K, Tomancak, P & Cardona, A. (2012): Fiji: an open–source platform for biological–image analysis. – Nature Methods 9: 676–682.

Singh, G.; Kukwa, M.; Dal Grande, F.; Łubek, A.; Otte, J. & Schmitt, I. (2019): A glimpse into genetic diversity and symbiont interaction patterns in lichen communities from areas with different disturbance histories in Białowieża forest, Poland. – Microorganisms 7: 335.

Škaloud, P.; Moya, P.; Molins, A.; Peksa, O.; Santos–Guerra, A. & Barreno, E. (2018): Untangling the hidden intrathalline microalgal diversity in *Parmotrema pseudotinctorum*: *Trebouxia crespoana* sp. nov. – The Lichenologist 50: 357–369.

Stamatakis, A. (2006): RAxML–VI–HPC: maximum likelihood–based phylogenetic analyses with thousands of taxa and mixed models. – Bioinformatics 22: 2688–2690.

Stamatakis, A.; Hoover, P. & Rougemont, J. (2008): A rapid bootstrap algorithm for the RAxML web servers. – Systematic Biology 57: 758–771.

Stirbet, A. & Govindjee (2011): On the relation between the kautsky effect (chorophyll *a* fluorescence induction and photosystem II: basic and applications of the OJIP fluorescent transient. – Journal of Photochemistry and Photobiology B: Biology 104: 236–257.

Tschermak–Woess, E. (1978): Über die Phycobionten der Sektion *Cystophora* von *Chaenotheca*, insbesondere *Dictyochloropsis splendida* und *Trebouxia simplex*, spec. nova: the phycobionts in the section *Cystophora* of *Chaenotheca*, especially *Dictyochloropsis splendida* and *Trebouxia simplex*, spec. nova. – Plant Systematics and Evolution 129: 185–208.

Vančurová, L.; Malíček, J.; Steinová, J. & Škaloud, P. (2021): Choosing the right life partner: ecological drivers of lichen symbiosis. – Frontiers in Microbiology 12: 769304.

Vančurová, L.; Muggia, L.; Peksa, O.; Řídká, T. & Škaloud, P. (2018): The complexity of symbiotic interactions influences the ecological amplitude of the host: a case study in *Stereocaulon* (lichenized *Ascomycota*). – Molecular Ecology 27: 3016–3033.

Veselá, V.; Malavasi, V. & Škaloud, P. (2024): A synopsis of green–algal lichen symbionts with an emphasis on their free–living lifestyle. – Phycologia 63: 317–338.

Zhao, X.; Fernández–Brime, S.; Wedin, M.; Locke, M.; Leavitt, S.D. & Lumbsch, H.T. (2017): Using multi–locus sequence data for addressing species boundaries in commonly accepted lichen–forming fungal species. – Organisms, Diversity and Evolution 17: 351–363.

Supplementary material

The following supplementary material is available for this article:

Supplementary Fig. S1, Fig. S2, Fig. S3, Fig. S4, Fig. S5.

Supplementary Table S1, Table S2, Table S3, Table S4.

This material is available as part of the online article (http://fottea.czechphycology.cz/contents)

Received April 24, 2024
Revised July 26, 2024
Accepted October 1, 2024
Prepublished online January 24, 2025